ACS chemical biology

Articles

pubs.acs.org/acschemicalbiology

Multicolor Monitoring of the Proteasome's Catalytic Signature

Melanie A. Priestman,[†] Qunzhao Wang,[†] Finith E. Jernigan,[†] Ruma Chowdhury,[‡] Marion Schmidt,[‡] and David S. Lawrence*[,†]

[†]Department of Chemistry, Division of Chemical Biology and Medicinal Chemistry, and Department of Pharmacology, University of North Carolina, Chapel Hill, North Carolina 27599, United States

[‡]Department of Biochemistry, Albert Einstein College of Medicine, Bronx, New York 10461, United States

Supporting Information

ABSTRACT: The proteasome, a validated anticancer target, participates in an array of biochemical activities, which range from the proteolysis of defective proteins to antigen presentation. We report the preparation of biochemically and photophysically distinct green, red, and far-red real-time sensors designed to simultaneously monitor the proteasome's chymotrypsin-, trypsin-, and caspase-like activities, respectively. These sensors were employed to assess the effect of simultaneous multiple active site catalysis on the kinetic properties of the individual subunits. Furthermore, we have found that the catalytic signature of the proteasome varies depending on the source, cell type, and disease state. Trypsin-like activity is more pronounced in yeast than in mammals, whereas chymotrypsin-like activity is the only activity detectable in B-cells (unlike other mammalian cells). Furthermore, chymotrypsin-like activity is more prominent in transformed B cells relative to their counterparts from healthy donors.

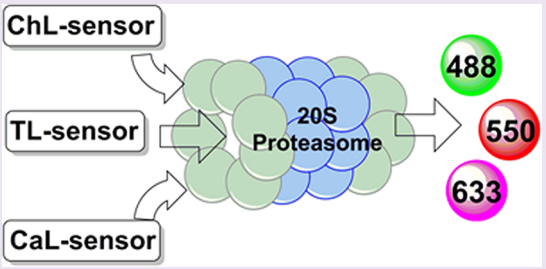

The proteasome serves as the primary proteolytic enzyme regulating the removal of polyubiquitinated proteins,[1,2] small monoubiquitinated proteins,[3] and peptides[4] in eukaryotic cells. Protein degradation is an essential participant in the immune response,[5] autophagy,[6] cardiac hypertrophy,[7] neurodegeneration,[8] and cancer.[9−11] The multisubunit proteasome contains a 20S core particle that is responsible for ATP-independent proteolysis of proteins. Associated regulator particles such as the 19S cap mediate deubiquitination, ATP-dependent substrate unfolding, and gate opening as well as access to the catalytic chamber of the proteasome core cylinder.[1] The 20S core particle is an assembly of two outer α-rings and 2 inner β-rings, each composed of 7 subunits. In the constitutive proteasome, found in all cells, each inner β-ring houses three distinct subunits that possess unique catalytic activities: caspase-like (CaL; β1 subunit), trypsin-like (TL; β2 subunit), and chymotrypsin-like (ChL; β5 subunit).[1] Each of the latter subunits can be replaced by the immunoproteasome subunits β1i, β2i, and β5i, resulting in either mixed proteasomes with one or two subunits replaced or the full immunoproteasome when all three are substituted.[12]

It is beginning to emerge that total proteasome activity and the ratios of the ChL, TL, and CaL activities, defined here as the proteasome catalytic signature, may vary depending on numerous factors. For example, proteasomes isolated from different species have altered processivity of proteins due to differences in catalytic rate of cleavage as well as turnover rates.[13] In addition, several laboratories have shown that proteasome composition and activity vary in different tissue and cell lines.[14,15] Even within a cell type there appears to be an assortment of factors that can alter proteasome activity such as age,[16] oxidative stress,[17] and disease state.[7−11] Furthermore, it has been suggested that ChL proteasome activity is elevated in cancer, although this proposal is controversial.[18−20] Furthermore, the importance of the proteasome's catalytic signature extends beyond a possible correlation between activity and cell type or disease state. For example, several antineoplastic agents that target the proteasome do so by interfering with ChL activity.[20] However, recent studies suggest that therapeutic efficacy may be enhanced by the presence of inhibitors that block CaL and TL activities as well.[21−24] In addition, clinical resistance to the proteasome inhibitor bortezomib has been at least partially ascribed to mutations in the ChL subunit.[25,26] Consequently, methods that furnish subunit-specific measurements of proteasome activity offer potential insight into the mechanism of action and resistance to current drugs as well as assistance in the identification of the appropriate drug cocktail.

The vast majority of kinetic studies carried out on the 20S proteasome have utilized fluorophore-labeled peptides that are biochemically acted upon by the individual active sites. However, these proteasome substrates employ luciferin[27] or fluorophores with similar photophysical properties, all of which are excited at wavelengths shorter than 400 nm.[4,28−30] Activity-based probes (ABPs), which target and covalently label the enzyme active site with a fluorophore, have also been described and used to assess the functional proteomics of the proteasome.[31−33] ABPs and fluorogenic substrates are comple-

Received: September 12, 2014
Accepted: October 24, 2014
Published: October 27, 2014

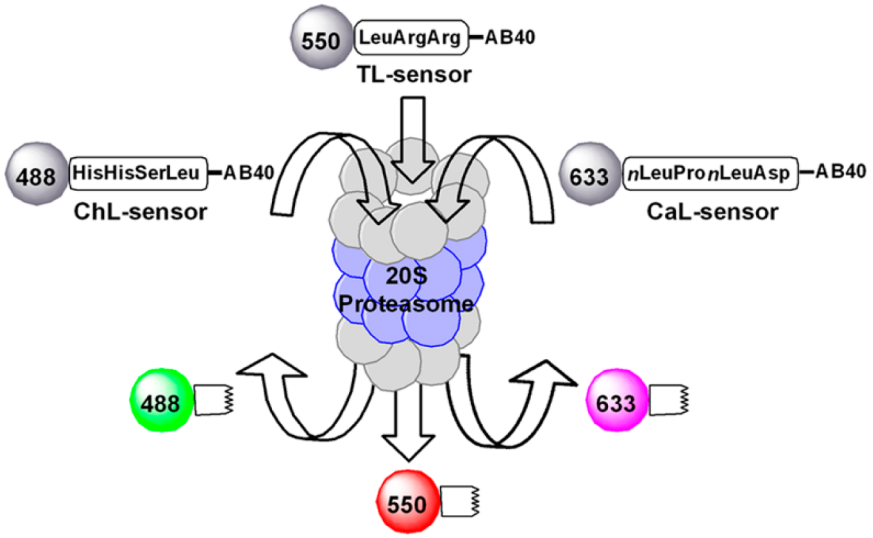

Figure 1. Multicolor monitoring of proteasome activity.

mentary methods that probe distinct elements of proteasome function.[33] There is considerable interest in identifying probes that discriminate between and simultaneously assess the catalytic subunits of the proteasome.[34−36] In this regard, we report the first example of a set of fluorescent real-time sensors capable of simultaneously monitoring all three of the catalytic activities of the proteasome and thereby furnish the catalytic signature of this multimeric multifunctional enzyme complex. We have found that catalytic activity in one subunit can be influenced by simultaneous activity in the other active sites. In addition, the catalytic signature varies in proteasomes isolated from different cell types and disease states and thus potentially serves as a fingerprint of the major source of proteolysis in cells.

RESULTS AND DISCUSSION

Design of Proteasome Sensors. Proteasome-specific monitoring of CaL, ChL, and TL enzymatic activities presents a number of molecular engineering challenges. First, the simultaneous assessment of three separate enzyme-catalyzed reactions requires the use of fluorophores with distinct photophysical properties. Second, these fluorophores must be embedded on substrates specific for the three individual catalytic entities of the proteasome. Although selective peptide-based substrates for CaL, ChL, and TL have been described, the luminescent readouts[4,37] for these sensors are identical and therefore preclude the ability to simultaneous measure the individual CaL, ChL, and TL protease activities. A wide variety of photophysically distinct fluorescent labels are available ranging in size from small well-defined fluorophores[38] to large nanoparticles.[39] Internally quenched peptides, species that contain a fluorophore on one end of the peptide chain and a fluorescent quencher on the other, have seen significant application as protease sensors.[39] Proteolysis liberates the fluorophore from the quencher and thereby furnishes a fluorescent readout. However, this approach poses additional challenges with respect to the proteasome since it potentially requires the identification of three distinct photophysically robust fluorophore/quencher pairs (i.e., relief of a deep fluorescent quench upon proteolysis). Furthermore, the fluorophore and quencher substituents would need to be readily accommodated within the proteasome's narrow central channel. We recently described a broad spectrum dark fluorescent quencher, a derivative of acid blue 40 (AB40), that can be used in conjunction with fluorophores that exhibit excitation wavelengths from 340 to 680 nm.[40] The broad spectral footprint of AB40 (Supporting Information Figure 1), along with its modest size, suggests that it might prove to be useful in providing the desired fluorescent sensors for each activity (Figure 1).

A small library of sensors was synthesized by appending photochemically distinct fluorophores to the N-terminus of the recognition sequences selective for each proteasomal activity (ChL, HHSL; TL, LRR; CaL, nLPnLD).[29] The fluorophore−peptide−AB40 sensors include fluorescein (FAM where λ_{ex} = 488 nm) for ChL, tetramethylrhodamine (TAMRA where λ_{ex} = 550 nm) for TL, and DyLight633 (λ_{ex} = 633) for CaL (Figure 2 and Supporting Information Figures 2−3). AB40 is appended to the side chain of the C-terminal lysine residue on each sensor.

Characterization of Proteasome Sensors. The kinetic rates of proteolysis and maximum fold fluorescent increases for the three sensors are listed in Table 1. ChL1−488 is rapidly

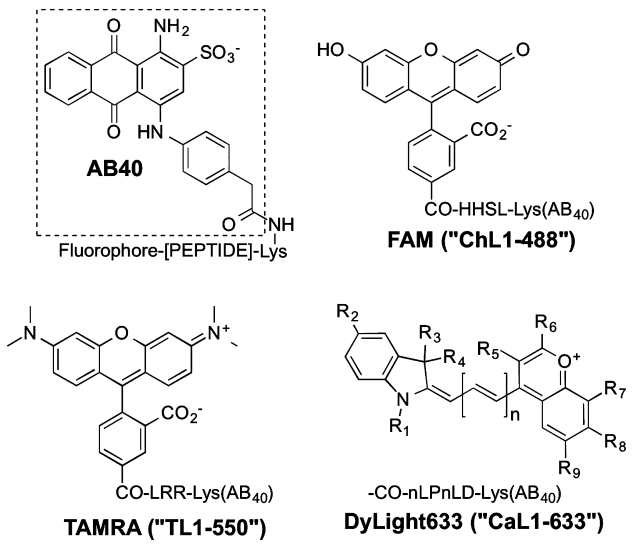

Figure 2. General structures of the proteasome sensors.

dx.doi.org/10.1021/cb5007322 | ACS Chem. Biol. 2015, 10, 433−440

Table 1. Characterization of Activity-Selective Proteasome Sensors

	specific activity (nmol min^{-1} mg^{-1} enzyme)		fold change	
proteasome sensor	2.5 μM	5 μM	2.5 μM	5 μM
FAM−HHSLK(AB40) ChL1−488	0.22 ± 0.02	0.31 ± 0.03	127 ± 2.6	137 ± 7.8
DyLight633−nLPnLDK(AB40) CaL1−633	0.03 ± 0.001	0.02 ± 0.002	32 ± 1.9	29 ± 0.2
TAMRA−LRRK(AB40) TL1−550	0.05 ± 0.003	0.06 ± 0.001	32 ± 2.9	31 ± 1.7

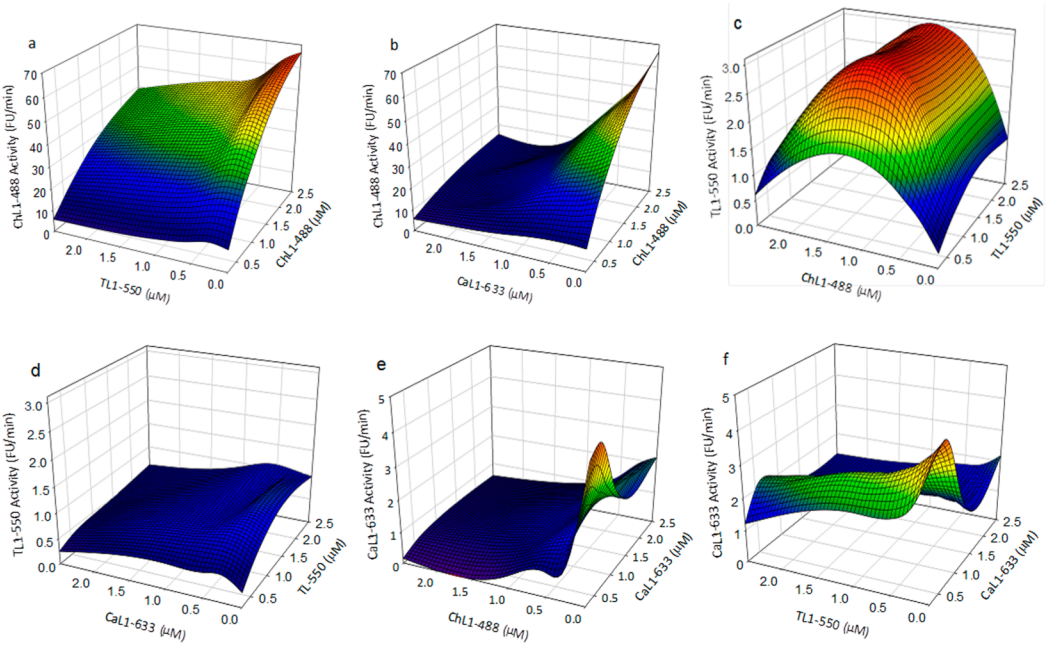

Figure 3. Optimization of the proteasome assay. Influence of each proteasome sensor on the activity of the other subunits. ChL1−488 activity with (a) TL1−550 or (b) CaL1−633; TL1−550 activity with (c) ChL1−488 or (d) CaL1−633; CaL1−633 activity with (e) ChL1−488 or (f) TL1−550.

hydrolyzed at all concentrations relative to that of its TL1−550 and CaL1−633 counterparts (Table 1). Efforts to improve the proteolysis rates by synthesizing peptides with different linkers between the peptide sequence and C-terminal Lys(AB40) resulted in nonspecific cleavage by the proteasome (data not shown). The K_m values were not determined because the sensors begin to aggregate at 10 μM, which is less than the presumed K_m.[4,29,30] Nonetheless, all sensors generate a robust fluorescent increase (30−140-fold) upon proteolysis.

We assessed the active site selectivity of each sensor using mutated proteasomes from yeast[41] as well as a variety of proteasome inhibitors with known active site preferences. All three catalytic β-subunits are synthesized as preproteins that require cleavage, exposing a critical N-terminal Thr residue important for catalytic activity. Deleted preprotein sequences are N$^{\alpha}$-acetylated, resulting in partial proteasome inactivation.[41,42] Four strains with such proteasome deletions were analyzed: CaL mutant, ChL mutant, TL mutant, and CaL + TL double deletion. We note that, although these deletions are known to result in a complete loss of CaL activity, only a partial loss in activity occurs with this mutation in the ChL and TL active sites.[41] In all instances, the rate of proteolysis of the sensors appropriately reflects the complete/partial loss of activity of the mutated proteasome catalytic sites (Supporting Information Table 1). For example, the CaL1−633 sensor is not proteolyzed by the proteasome containing the mutation in the CaL subunit, but it is cleaved by proteasomes containing the same mutations in either the ChL or TL subunit. A further assessment of the selectivity of each sensor was accomplished by using the proteasome inhibitors Ac-APnLD-aldehyde (CaL inhibitor),[29] epoxomicin (ChL inhibitor),[43] MG132 (ChL and CaL inhibitor),[44] and TLCK (TL inhibitor).[45] Each inhibitor was preincubated with the proteasome in order to form either a covalent or reversible adduct within the targeted active site. As expected, the CaL-targeted Ac-APnLD-aldehyde (IC_{50} = 2.3 ± 0.6 μM) and MG132 (IC_{50} = 180 ± 150 μM) both inhibit CaL1−633 proteolysis (Supporting Information Figures 5−8 and Table 2). Proteolysis of the ChL sensor, ChL1−488, is inhibited by the ChL-targeted inhibitors epoxomicin (IC_{50} = 0.08 ± 0.03 μM) and MG132 (IC_{50} = 0.62 ± 0.06 μM). Finally, hydrolysis of the TL sensor, TL1−550, is compromised by the TL-directed inhibitor TLCK (IC_{50} = 210 ± 20 μM). In summary, the ChL-, TL-, and CaL-targeted sensors selectively detect, in the expected fashion, the loss of specific active site activity due to mutation or added inhibitor with known active site selectivity.

Simultaneous Monitoring of Proteasome Activities. We optimized the conditions for simultaneously monitoring all three proteasomal activities by first assessing the conditions for two-site multicolor visualization (i.e., ChL + TL; CaL + TL; CaL + ChL). This multistep process is critical since occupancy at one active site can influence the catalytic activity at a second active site.[28,35] Indeed, the rate of proteolysis of ChL1−488 is reduced by up to 50% in the presence of TL1−550 and up to 90% in the presence of CaL1−633 (Figure 3a,b). These observations appear to be consistent with studies by Kisselev and colleagues who found that inhibitors of CaL and TL sites sensitize cells to inhibitors that target ChL sites.[21,23] Perhaps

dx.doi.org/10.1021/cb5007322 | ACS Chem. Biol. 2015, 10, 433−440

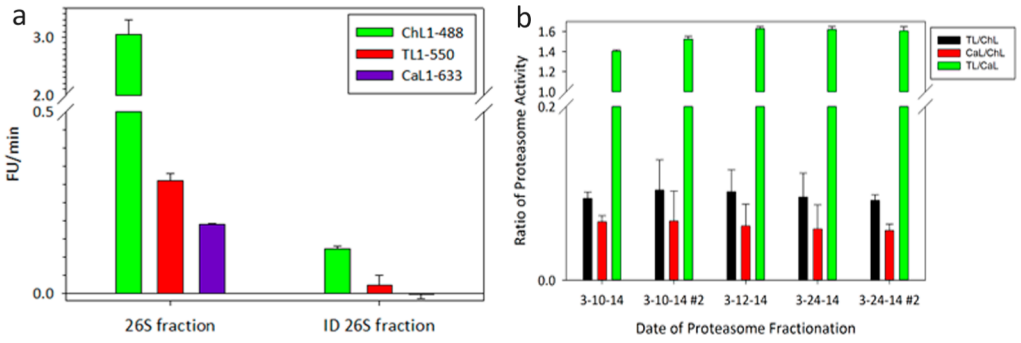

Figure 4. Proteasome signature of HeLa cells. (a) Activity of proteasome from HeLa cells with ChL1−488, TL1−550, and CaL1−633 sensors. The 26S fraction is the resuspended pellet after ultracentrifugation containing the proteasome and the ID 26S fraction is the immunodepleted 26S fraction. (b) Reproducibility of the ratios of proteasome activity from HeLa cell ultracentrifugation fractions.

not surprisingly, CaL activity is likewise suppressed in the presence of the ChL substrate (Figure 3e). However, quite unexpectedly, we found that the rate of TL1−550 hydrolysis is actually enhanced (up to 5-fold) when ChL1−488 is present (Figure 3c). Finally, TL activity is reduced in the presence of CaL1−633, and CaL activity is impaired in the presence of TL1−550 (Figure 3d,f). These results highlight the intricate enzymological relationships of the individual proteolytic active sites of the proteasome.

We subsequently evaluated the simultaneous three-color monitoring of all proteasomal hydrolytic activities (Supporting Information Figure 9) and identified optimized sensor concentrations (0.5 μM ChL1−488, 1.0 μM TL1−550, and 1.0 μM CaL1−633; Supporting Information Figure 10). Under these conditions, ChL1−488 is cleaved substantially faster than that of TL1−550 and CaL1−633. However, the kinetic activity for all three sensors is readily and reproducibly measured. We once again utilized impaired proteasomes from yeast and a variety of active site-selective inhibitors to verify that each sensor monitors its designated proteasome activity. The sensors detect the loss of activity in the yeast deletions in the expected active site-selective fashion (Supporting Information Table 3). Furthermore, incubation of wild-type proteasome with CaL-targeted Ac-APnLD-aldehyde or MG132 (high concentrations) impairs CaL1−633 cleavage, ChL-directed epoxomicin or MG132 (low or high concentration) inhibits ChL1−488 proteolysis (Supporting Information Figure 11), and the combination of CaL inhibitor Ac-APnLD-aldehyde and ChL-inhibitor epoxomicin blocks both ChL and CaL activities.

Multicolor Proteasome Sensor Assay: Proteasome Catalytic Signature. Confirmation that these sensors can yield an assessment of the proteasome catalytic activities from cell cultures was performed by using isolated proteasomes from HeLa cells that are devoid of other proteases.[4] This protocol employs a cytosolic lysate that is generated upon incubation with digitonin, followed by centrifugation, thereby separating proteins associated with membranes (cell membrane fraction). The cytosolic fraction is subjected to ultracentrifugation, thereby pelleting the proteasome (cytosolic supernatant and cytosolic pellet) (Supporting Information Figure 12). Testing of the membrane and cytosolic supernatant fractions with ChL1−488, TL1−550, and CaL1−633 indicated cleavage of all sensors. The most likely explanation for this is the presence of other proteases in these fractions because immunodepletion with a 20S core particle antibody only slightly reduced the activities (data not shown). However, greater than 95% of the cytosolic pellet activity is exclusively due to the proteasome, which can be removed by immunodepletion (Figure 4a). Furthermore, we were able to reproducibly acquire TL/ChL, CaL/ChL, and TL/CaL catalytic ratios from HeLa cells (Figure 4b). One major advantage of the single-well three-sensor assay is that the ratios are independent of the amount of proteasome present and therefore create consistent data that is easily evaluated for comparison between separate samples.

Does the Proteasome Catalytic Signature Vary among Different Species and Cell Types? The proteasome is found in all eukaryotes and some prokaryotes. Not surprisingly, significant structural and enzymological differences exist between and within individual species. For example, proteasomal processivity, the degree to which substrates are degraded to small peptides, increases as a function of increasing species complexity.[13] Furthermore, differences have been noted in proteasome subunit activity in different tissue types[14] and cell lines[15,46] as well as in primary cells from different leukemia patients.[20] As a preliminary survey, we examined ChL, CaL, and TL activities from several purified sources (yeast, rabbit, and human constitutive and immunoproteasomes; Figure 5). All of the proteasome sources hydrolyze ChL1−488 most rapidly, followed by TL1−550 and then CaL1−633 (data not shown). However, this ordered ranking of activities does not necessarily provide a quantitative assessment of the inherent catalytic prominence of the respective active sites. Indeed, although ChL

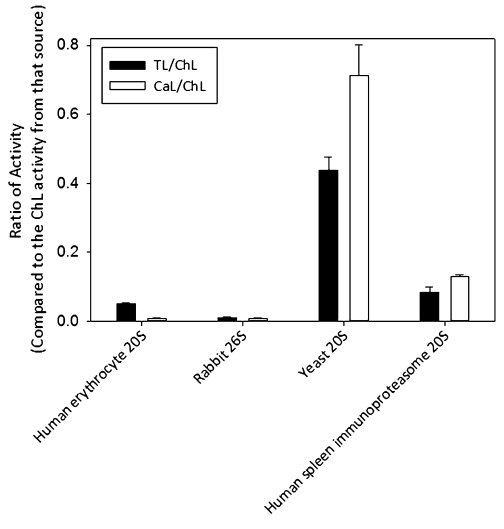

Figure 5. Proteasome catalytic signatures, ratios of ChL/TL and ChL/CaL, vary from different species and sources.

dx.doi.org/10.1021/cb5007322 | ACS Chem. Biol. 2015, 10, 433−440

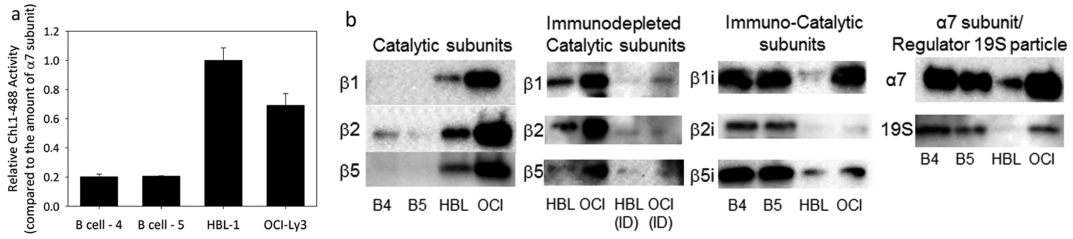

Figure 6. Proteasome catalytic signature and subunit composition from B-cells. (a) Relative proteasome ChL1−488 activity from B-cells. (b) Western blots showing the different subunit composition of the proteasome in the different B-cell lines. B4 and B5 are normal B-cells from health donors, HBL-1 and OCI-Ly3 are cancerous B-cell lines, and HBL-1 ID and OCI-Ly3 ID are the corresponding immunodepleted samples.

activity is commonly thought to be preeminent in terms of protein degradation,[4] the importance of the TL and CaL sites has recently garnered significant attention.[21,23,47] The proteasome sensor set developed in this study provides a comparative assessment of differences in these activities, thereby potentially offering insight into enzymatic variations among species as well as between normal and diseased cell types. In the latter case, this may ultimately offer possible therapeutic opportunities with respect to proteasomal targeting. The catalytic activities for the various sources reveal significant differences (Figure 5). In particular, the TL activity is more pronounced (versus ChL and CaL) in yeast proteasome than the corresponding TL activity from mammalian sources (Figure 5). The human erythrocyte constitutive proteasome (β1, β2, and β5) exhibits TL/ChL and CaL/ChL ratios that are 2 and 10 times lower, respectively, than the ratios from the immunoproteasome (β1i, β2i, and β5i) purified from human spleen.

Does the Proteasome Catalytic Signature Vary by Disease State? The FDA approval of bortezomib in 2003 and carfilzomib in 2012 to treat multiple myeloma and, in the case of bortezomib, mantle cell lymphoma (a subtype of B-cell lymphoma) illustrates the efficacy of anticancer agents that inhibit the ChL activity of the proteasome.[48] Bortezomib and other proteasome inhibitors are also currently being tested in combination therapy for numerous B-cell lymphomas.[49] Consequently, we opted to test the proteasome sensors in several cancerous B-cell lines as well as from normal B-cells from healthy donors. Unlike HeLa cell lysates, where all three proteolytic activities are easily distinguished, ChL activity is the only measurable activity in proteasomes from normal B-cells (Supporting Information Figure 13). Furthermore, ChL proteasomal activity dwarfs the observed TL and CaL activities in proteasomes isolated from the cancerous B-cell lines HBL-1 and OCl-Ly3 (Supporting Information Figure 13). However, relative ChL activity, when compared to the total amount of proteasome, as assessed by the amount of α7 proteasome subunit present, is 3−5-fold higher in the cancerous B-cell lines than that in normal B-cells (Figure 6a). We also found that normal B-cells predominantly express the immunoproteasome catalytic subunits (β1i, β2i, and β5i), whereas, the cancerous B-cell lines possess both the constitutive (β1, β2, and β5) and the immunoproteasome catalytic subunits (Figure 6b).

Distinctive proteasome activity has been reported by others, suggesting that ChL activity is higher in cancerous cells lines;[18,19] however, Driessen et al. failed to observe any correlation between ChL activity and cancer in leukemia patients.[20] In addition, other studies suggest that bortezomib resistance occurs in cells with high ChL and CaL activities.[20,26] While all of these studies have utilized APBs and/or short-wavelength peptide sensors to show important differences in proteasome activity and responses to inhibitors, we believe that the sensor set developed here provides a needed approach that allows for real-time analysis of all three proteolytic activities. The use of APBs has proven to be a powerful tool for isolating and identifying proteases that are in an active state both in cell lysates and in cell culture.[50] Fluorescently tagged APBs have been critical in understanding protease activation at the subcellular level.[50] Furthermore, ABPs have successfully been used in drug development for identifying inhibitors.[50] APBs for the proteasome have been utilized to distinguish activation of the constitutive proteasome (β1, β2, and β5) versus the immunoproteasome (β1i, β2i, and β5i) as well as establishing which subunits are inhibited in cells by anticancer agents such as bortezomib.[32] However, there are limitations of APBs that can be addressed with peptide sensors. Proteasome activity is known to be effected by subunit composition as well as numerous regulatory proteins. Therefore, APBs that monitor the amount of catalytically competent enzyme at a single time point[50] do not furnish an understanding of how enzymatic activity is altered by regulatory proteins or post-translational modifications. The peptide sensors described here are not specific for the proteasome over other proteases but do provided a direct measure of the levels of enzymatic activity when working with lysates or purified samples. Unlike APBs, fluorescent peptide sensors amplify the signal and can therefore be used with smaller concentrations of enzymes for real-time monitoring of enzymatic activity. Although short-wavelength peptides are available for monitoring the individual activities of the proteasome, there are no peptide sensors that permit the monitoring of all activities in a single assay, thereby affording a true understanding of the proteasome catalytic efficiency. Although the sensors described in this study are sufficient for use with isolated proteasomes, live cell studies will require the development of proteasome-selective analogues. In addition, live cell imaging of enzymatic activity necessitates a well-defined start point. This may be feasible using light-activated derivatives of these sensors by employing a strategy analogous to a previously described approach.[51]

The proteasome is responsible for the proteolytic breakdown of polyubiquitinated proteins in all cells. It plays important roles in protein turnover, cell division, autophagy, and antigen presentation. In addition, altered proteasome function has been linked to aging, cardiac hypertrophy, neurodegeneration, and cancer. Therefore, methods to monitor the three proteolytic activities (the "catalytic signature") of the proteasome are necessary for understanding such processes. We have described a proteasome sensor triad for the simultaneous fluorescent monitoring all three proteasomal protease activities. These sensors were used to demonstrate that the catalytic signature of the proteasome is unique to each cell line. Furthermore, in B-

dx.doi.org/10.1021/cb5007322 | ACS Chem. Biol. 2015, 10, 433−440

cells, only ChL activity is detectable, and cultured cancerous B-cells have higher ChL activity than in normal B-cells. The simultaneous monitoring of the multiple activities of the proteasome offers the ability to assess the proteasome catalytic signature, which could prove to be a barometer of various cellular and diseased states.

METHODS

Materials. Rabbit proteasome fraction II was purchased from Sigma. Human erythrocyte 26S proteasome and human spleen immunoproteasome 20S were purchased from Enzo Life Sciences. Purified rabbit 20S proteasome was purchased from Calbiochem. All Proteasome inhibitors were purchased from Enzo Life Sciences. HeLa cells were purchased from the tissue culture facility at the University of North Carolina. Normal B-cells were purchased from AllCells. OCI-Ly3 and HBL-1 cells were provided by Dr. Ben Major in the Department of Cell Biology and Physiology at the University of North Carolina. The BCA kit (Thermo Scientific) was used to quantify the protein content of all lysates. All other chemicals were from Fisher or Sigma unless otherwise noted.

Assessment of Proteasome Activity. All data is reported as the mean ± standard deviation of triplicate assays, where FU is fluorescent units.

Rates and Fold Changes. The activities of all proteasomes were determined in assay buffer (50 mM Tris, pH 7.5, 40 mM KCl, 4 mM $MgCl_2$, 1 mM ATP, 1 mM EDTA) and 0.05% bovine serum albumin (BSA)[4] with 0−5 μM of each proteasome sensor. The reactions were initiated with 1−40 μg of proteasome, and the reaction progress was monitored for 2 h at RT unless otherwise noted. For determination of the fluorescent fold change, each reaction was spiked with 10 μg of rabbit fraction II proteasome and incubated at RT overnight. Control assays without proteasome were run to ensure that the fluorescent change was due to proteasome activity and not hydrolysis. Fluorescence was monitored on Molecular Devices Spectra Max Gemini EM plate reader with excitation at 490, 550, and 625 nm, with emission at 515, 575, and 655 nm, respectively. SigmaPlot 12 (775206611) was used for the analysis of all data. The rate of each assay was determined using a linear fit to the first 10% of substrate consumption. Fold changes were determined by dividing the final fluorescence by the initial fluorescence. Conversion of fluorescence change to micromoles of product formed was determined by assuming that the reaction was 95% complete after determining the fold change. A linear fit was then applied to the fluorescence at 0, 1, 2.5, and 5 μM, allowing the conversion from fluorescent units to micromoles.

Inhibition. Unless otherwise noted, 5.5 μg of rabbit proteasome fraction II was preincubated with inhibitor in assay buffer at 37 °C for 30 min. The reaction was initiated with 0−5 μM proteasome sensor. Activity was measured as described above. For *N*-α-tosyl-L-lysinyl-chloromethylketone (TLCK) inhibition, 5.5 μg of rabbit proteasome fraction II or 7.8 μg of control yeast deficient lysate was incubated with TLCK in buffer, pH 5.5, at 37 °C for 30 min. The incubation was diluted 1:10 in assay buffer, and the reaction was initiated with 0−5 μM proteasome sensors. All data was fit to the standard IC_{50} equation and plotted using SigmaPlot.

Yeast Proteasome Activity-Deficient Lysates. Harvested cells expressing proteasome-deficient mutants were purified as described recently.[41,52] Cells were drop-frozen in liquid nitrogen, and lysis was carried out by cryomilling. The corresponding powders were stored at −80 °C. Lysates were resuspended in assay buffer on ice for 10 min and centrifuged at 10 000*g* at 4 °C for 30 min. The lysate protein concentration was determined using the BCA assay. Proteasome assays were run as described above for the rates with 34 μg of each lysate. The rate of each assay was determined using a linear fit to the first 10% of substrate consumption.

Cell Culture. HeLa cells were passaged by treatment with 0.5% trypsin + 0.53 mM EDTA before reaching confluence and maintained in DMEM containing 10% fetal bovine serum (FBS), nonessential amino acids, and penicillin−streptomycin at 37 °C in a 5% CO_2 incubator. HBL-1 and OCI-Ly3 cells were maintained between 3×10^5 and 1×10^6 in RPMI 1640 media containing 15% FBS supplemented with penicillin−streptomycin at 37 °C in a 5% CO_2 incubator.

Proteasome-Enriched Cell Extracts. One 90% confluent 75 cm^2 flask of HeLa cells or 25 mL of HBL-1 or OCI-Ly3 cells at 6×10^5 were used to isolate a cell fraction to monitor proteasome activity while removing other protease activity.[4] Isolated cells were resuspended in ice-cold PBS and centrifuged at 1000*g* for 5 min at 4 °C for 3 cycles. Cells were then resuspended in 4 volumes homogenization buffer (50 mM Tris, 250 mM sucrose, 5 mM $MgCl_2$, 1 mM ATP, 1 mM DTT, 0.5 mM EDTA, pH 7.5) with 0.025% digitonin and incubated on ice for 10 min, followed by centrifugation at 17 000*g* for 10 min at 4 °C. The supernatant was then ultracentrifuged at 180 000*g* for 4 h at 4 °C. The supernatant was removed, and the pellet was resuspended in homogenization buffer. Protein concentration was determined using the BCA kit from Thermo Scientific.

Immunodepletion and Western Blots. Proteasome 20S core subunits, 20S β1, 20S β2, 20S β5, 20S α7, and 11S α, and 19S ADRM1 antibodies were purchased from Enzo Life Sciences. Proteasome 20S β1i and 20S β5i antibodies were purchased from Thermo Fisher Scientific. Proteasome 20S β2i antibody was purchased from NovusBio. All secondary antibodies were purchased from GE Healthcare.

Immunodepletion of proteasome from cell lysates was accomplished by incubating lysates (1 mg) with 20 μL of proteasome 20S core subunits primary antibody at 4 °C overnight. The mixture was added to 200 μL of Protein A-sepharose 4B beads from Invitrogen (prewashed with homogenization buffer), incubated for 1 h at 4 °C, and loaded in a spin column, and the supernatant was collected as the immunodepleted fraction. Immunodepletion was confirmed by western blot. Quantification of the immunodepletion was performed using ImageJ software.

Western blots of all samples, 50 μg per well, were performed on 4−20% SDS Tris-HCl gels (BioRad) and transferred to nitrocellulose membranes. Membranes were blocked with 5% BSA in PBS + 0.1% Tween-20 for 2 h before incubation with 1:500 of the primary antibody in the blocking solution at 4 °C overnight. Membranes were washed with PBS + 0.1% Tween-20, incubated with 1:5000 secondary HRP conjugated antibody for 2 h, and washed with PBS. Visualization was performed according to Pierce's recommended protocols for their ECL Pico kit. Images were acquired using an Alpha Innotech Fluorchem FC2 using the chemiluminescent settings.

Proteasome Assays with Cell Lysates. The activity of all cell lysates and immunodepleted samples was determined in assay buffer with 0.05% BSA and 0.5 μM ChL1−488, 1 μM TL1−550, and 1 μM CaL1−633. The reactions were initiated with 10 μg of cell lysate, and the reaction progress was monitored for 2 h at RT. Control assays without cell lysate were run to ensure that the fluorescent change was due to proteasome activity and not hydrolysis. Fluorescence was monitored on Molecular Devices Spectra Max Gemini EM plate reader with excitation at 490, 550, and 625 nm and emission at 515, 575, and 655 nm, respectively. SigmaPlot was used for the analysis of all data. The rate of each reaction was determined using a linear fit to the first 10% of substrate consumption.

ASSOCIATED CONTENT

Supporting Information

Synthetic methods. Table S1: Rate of cleavage by yeast deficient lysates for all proteasome sensors. Table S2: Inhibition values for all proteasome sensors. Table S3: Rate of cleavage by yeast deficient lysates for all proteasome sensors. Figure S1: Relative absorbance spectra of AB40, ChL1−488, TL1−550, and CaL1−633. Figure S2: Mass spectra for ChL1−488, TL1−550, and CaL−633. Figure S3: Reverse-phase HPLC traces of purified ChL1−488, TL1−550, and CaL1−633. Figure S4: Representative fluorescent curves for ChL1−488, TL1−550, and CaL1−633 cleavage by the proteasome. Figure S5: Inhibition of proteasome-catalyzed hydrolysis of proteasome

sensors by the CaL inhibitor Ac-APnLD-aldehyde. Figure S6: Inhibition of proteasome-catalyzed hydrolysis of proteasome sensors by the ChL inhibitor epoxomicin. Figure S7: Inhibition of proteasome-catalyzed hydrolysis of proteasome sensors by the ChL/CaL inhibitor MG132. Figure S8: Inhibition of proteasome-catalyzed hydrolysis of proteasome sensors by the TL inhibitor TLCK. Figure S9: Optimization of proteasome assays with three proteasome sensors. Figure S10: Representative fluorescent curves for the three-color proteasome assay. Figure S11: Inhibition of specific activities of the proteasome. Figure S12: Protease activity toward ChL1−488, TL1−550, and CaL1−633 sensors from HeLa cell fractionation. Figure S13: B-cell proteasome activity toward ChL1−488, TL1−550, and CaL1−633 sensors. This material is available free of charge via the Internet at http://pubs.acs.org.

AUTHOR INFORMATION

Corresponding Author

*E-mail: lawrencd@email.unc.edu.

Notes

The authors declare no competing financial interest.

ACKNOWLEDGMENTS

We thank M. Cann for maintaining the HBL-1 and OCI-Ly3 cell lines. We thank the National Institutes of Health for financial support (RO1 CA79954 to D.S.L. and RO1 GM084228 to M.S.).

REFERENCES

(1) Marques, A. J., Palanimurugan, R., Matias, A. C., Ramos, P. C., and Dohmen, R. J. (2009) Catalytic mechanism and assembly of the proteasome. *Chem. Rev. 109*, 1509−1536.

(2) Strieter, E. R., and Korasick, D. A. (2012) Unraveling the complexity of ubiquitin signaling. *ACS Chem. Biol. 7*, 52−63.

(3) Abeywardana, T., Lin, Y. H., Rott, R., Engelender, S., and Pratt, M. R. (2013) Site-specific differences in proteasome-dependent degradation of monoubiquitinated alpha-synuclein. *Chem. Biol. 20*, 1207−1213.

(4) Kisselev, A. F., and Goldberg, A. L. (2005) Monitoring activity and inhibition of 26S proteasomes with fluorogenic peptide substrates. *Methods Enzymol. 398*, 364−378.

(5) Basler, M., Kirk, C. J., and Groettrup, M. (2013) The immunoproteasome in antigen processing and other immunological functions. *Curr. Opin. Immunol. 25*, 74−80.

(6) Wang, X. J., Yu, J., Wong, S. H., Cheng, A. S., Chan, F. K., Ng, S. S., Cho, C. H., Sung, J. J., and Wu, W. K. (2013) A novel crosstalk between two major protein degradation systems: regulation of proteasomal activity by autophagy. *Autophagy 9*, 1500−1508.

(7) Day, S. M. (2013) The ubiquitin proteasome system in human cardiomyopathies and heart failure. *Am. J. Physiol.: Heart Circ. Physiol. 304*, H1283−1293.

(8) Dennissen, F. J., Kholod, N., and van Leeuwen, F. W. (2012) The ubiquitin proteasome system in neurodegenerative diseases: culprit, accomplice or victim? *Prog. Neurobiol 96*, 190−207.

(9) Adams, J. (2004) The proteasome: a suitable antineoplastic target. *Nat. Rev. Cancer 4*, 349−360.

(10) Schmidt, M., and Finley, D. (2014) Regulation of proteasome activity in health and disease. *Biochim. Biophys. Acta 1843*, 13−25.

(11) Yang, H., Zonder, J. A., and Dou, Q. P. (2009) Clinical development of novel proteasome inhibitors for cancer treatment. *Expert Opin. Invest. Drugs 18*, 957−971.

(12) Liggett, A., Crawford, L. J., Walker, B., Morris, T. C., and Irvine, A. E. (2010) Methods for measuring proteasome activity: current limitations and future developments. *Leuk. Res. 34*, 1403−1409.

(13) Kraut, D. A., Israeli, E., Schrader, E. K., Patil, A., Nakai, K., Nanavati, D., Inobe, T., and Matouschek, A. (2012) Sequence- and species-dependence of proteasomal processivity. *ACS Chem. Biol. 7*, 1444−1453.

(14) Berkers, C. R., van Leeuwen, F. W., Groothuis, T. A., Peperzak, V., van Tilburg, E. W., Borst, J., Neefjes, J. J., and Ovaa, H. (2007) Profiling proteasome activity in tissue with fluorescent probes. *Mol. Pharmaceutics 4*, 739−748.

(15) Fabre, B., Lambour, T., Garrigues, L., Ducoux-Petit, M., Amalric, F., Monsarrat, B., Burlet-Schiltz, O., and Bousquet-Dubouch, M. P. (2014) Label-free quantitative proteomics reveals the dynamics of proteasome complexes composition and stoichiometry in a wide range of human cell lines. *J. Proteome Res. 13*, 3027−3037.

(16) Tomaru, U., Takahashi, S., Ishizu, A., Miyatake, Y., Gohda, A., Suzuki, S., Ono, A., Ohara, J., Baba, T., Murata, S., Tanaka, K., and Kasahara, M. (2012) Decreased proteasomal activity causes age-related phenotypes and promotes the development of metabolic abnormalities. *Am. J. Pathol. 180*, 963−972.

(17) Keller, J. N., Huang, F. F., Zhu, H., Yu, J., Ho, Y. S., and Kindy, T. S. (2000) Oxidative stress-associated impairment of proteasome activity during ischemia−reperfusion injury. *J. Cereb. Blood Flow Metab. 20*, 1467−1473.

(18) Frisan, T., Levitsky, V., and Masucci, M. G. (2000) Variations in proteasome subunit composition and enzymatic activity in B-lymphoma lines and normal B cells. *Int. J. Cancer 88*, 881−888.

(19) Masdehors, P., Merle-Beral, H., Maloum, K., Omura, S., Magdelenat, H., and Delic, J. (2000) Deregulation of the ubiquitin system and p53 proteolysis modify the apoptotic response in B-CLL lymphocytes. *Blood 96*, 269−274.

(20) Kraus, M., Ruckrich, T., Reich, M., Gogel, J., Beck, A., Kammer, W., Berkers, C. R., Burg, D., Overkleeft, H., Ovaa, H., and Driessen, C. (2007) Activity patterns of proteasome subunits reflect bortezomib sensitivity of hematologic malignancies and are variable in primary human leukemia cells. *Leukemia 21*, 84−92.

(21) Britton, M., Lucas, M. M., Downey, S. L., Screen, M., Pletnev, A. A., Verdoes, M., Tokhunts, R. A., Amir, O., Goddard, A. L., Pelphrey, P. M., Wright, D. L., Overkleeft, H. S., and Kisselev, A. F. (2009) Selective inhibitor of proteasome's caspase-like sites sensitizes cells to specific inhibition of chymotrypsin-like sites. *Chem. Biol. 16*, 1278−1289.

(22) Chauhan, D., Catley, L., Li, G., Podar, K., Hideshima, T., Velankar, M., Mitsiades, C., Mitsiades, N., Yasui, H., Letai, A., Ovaa, H., Berkers, C., Nicholson, B., Chao, T. H., Neuteboom, S. T., Richardson, P., Palladino, M. A., and Anderson, K. C. (2005) A novel orally active proteasome inhibitor induces apoptosis in multiple myeloma cells with mechanisms distinct from bortezomib. *Cancer Cell 8*, 407−419.

(23) Mirabella, A. C., Pletnev, A. A., Downey, S. L., Florea, B. I., Shabaneh, T. B., Britton, M., Verdoes, M., Filippov, D. V., Overkleeft, H. S., and Kisselev, A. F. (2011) Specific cell-permeable inhibitor of proteasome trypsin-like sites selectively sensitizes myeloma cells to bortezomib and carfilzomib. *Chem. Biol. 18*, 608−618.

(24) Geurink, P. P., van der Linden, W. A., Mirabella, A. C., Gallastegui, N., de Bruin, G., Blom, A. E., Voges, M. J., Mock, E. D., Florea, B. I., van der Marel, G. A., Driessen, C., van der Stelt, M., Groll, M., Overkleeft, H. S., and Kisselev, A. F. (2013) Incorporation of non-natural amino acids improves cell permeability and potency of specific inhibitors of proteasome trypsin-like sites. *J. Med. Chem. 56*, 1262−1275.

(25) Franke, N. E., Niewerth, D., Assaraf, Y. G., van Meerloo, J., Vojtekova, K., van Zantwijk, C. H., Zweegman, S., Chan, E. T., Kirk, C. J., Geerke, D. P., Schimmer, A. D., Kaspers, G. J., Jansen, G., and Cloos, J. (2012) Impaired bortezomib binding to mutant beta5 subunit of the proteasome is the underlying basis for bortezomib resistance in leukemia cells. *Leukemia 26*, 757−768.

(26) Kale, A. J., and Moore, B. S. (2012) Molecular mechanisms of acquired proteasome inhibitor resistance. *J. Med. Chem. 55*, 10317−10327.

(27) Moravec, R. A., O'Brien, M. A., Daily, W. J., Scurria, M. A., Bernad, L., and Riss, T. L. (2009) Cell-based bioluminescent assays for

all three proteasome activities in a homogeneous format. *Anal. Biochem. 387*, 294−302.
(28) Kisselev, A. F., Akopian, T. N., Castillo, V., and Goldberg, A. L. (1999) Proteasome active sites allosterically regulate each other, suggesting a cyclical bite−chew mechanism for protein breakdown. *Mol. Cell 4*, 395−402.
(29) Kisselev, A. F., Garcia-Calvo, M., Overkleeft, H. S., Peterson, E., Pennington, M. W., Ploegh, H. L., Thornberry, N. A., and Goldberg, A. L. (2003) The caspase-like sites of proteasomes, their substrate specificity, new inhibitors and substrates, and allosteric interactions with the trypsin-like sites. *J. Biol. Chem. 278*, 35869−35877.
(30) Orlowski, M., Cardozo, C., Hidalgo, M. C., and Michaud, C. (1991) Regulation of the peptidylglutamyl-peptide hydrolyzing activity of the pituitary multicatalytic proteinase complex. *Biochemistry 30*, 5999−6005.
(31) Bogyo, M. (2005) Screening for selective small molecule inhibitors of the proteasome using activity-based probes. *Methods Enzymol. 399*, 609−622.
(32) Berkers, C. R., Verdoes, M., Lichtman, E., Fiebiger, E., Kessler, B. M., Anderson, K. C., Ploegh, H. L., Ovaa, H., and Galardy, P. J. (2005) Activity probe for *in vivo* profiling of the specificity of proteasome inhibitor bortezomib. *Nat. Methods 2*, 357−362.
(33) Li, N., Kuo, C. L., Paniagua, G., van den Elst, H., Verdoes, M., Willems, L. I., van der Linden, W. A., Ruben, M., van Genderen, E., Gubbens, J., van Wezel, G. P., Overkleeft, H. S., and Florea, B. I. (2013) Relative quantification of proteasome activity by activity-based protein profiling and LC-MS/MS. *Nat. Protoc. 8*, 1155−1168.
(34) Verdoes, M., Willems, L. I., van der Linden, W. A., Duivenvoorden, B. A., van der Marel, G. A., Florea, B. I., Kisselev, A. F., and Overkleeft, H. S. (2010) A panel of subunit-selective activity-based proteasome probes. *Org. Biomol. Chem. 8*, 2719−2727.
(35) Wakata, A., Lee, H. M., Rommel, P., Toutchkine, A., Schmidt, M., and Lawrence, D. S. (2010) Simultaneous fluorescent monitoring of proteasomal subunit catalysis. *J. Am. Chem. Soc. 132*, 1578−1582.
(36) Carmony, K. C., and Kim, K. B. (2013) Activity-based imaging probes of the proteasome. *Cell Biochem. Biophys. 67*, 91−101.
(37) Moravec, R. A., O'Brien, M. A., Daily, W. J., Scurria, M. A., Bernad, L., and Riss, T. L. (2009) Cell-based bioluminescent assays for all three proteasome activities in a homogeneous format. *Anal. Biochem. 387*, 294−302.
(38) Lavis, L. D., and Raines, R. T. (2008) Bright ideas for chemical biology. *ACS Chem. Biol. 3*, 142−155.
(39) Wysocka, M., and Lesner, A. (2013) Future of protease activity assays. *Curr. Pharm. Des 19*, 1062−1067.
(40) Jernigan, F. E., and Lawrence, D. S. (2013) A broad spectrum dark quencher: construction of multiple colour protease and photolytic sensors. *Chem. Commun. 49*, 6728−6730.
(41) Arendt, C. S., and Hochstrasser, M. (1999) Eukaryotic 20S proteasome catalytic subunit propeptides prevent active site inactivation by N-terminal acetylation and promote particle assembly. *EMBO J. 18*, 3575−3585.
(42) Schmidtke, G., Kraft, R., Kostka, S., Henklein, P., Frommel, C., Lowe, J., Huber, R., Kloetzel, P. M., and Schmidt, M. (1996) Analysis of mammalian 20S proteasome biogenesis: the maturation of beta-subunits is an ordered two-step mechanism involving autocatalysis. *EMBO J. 15*, 6887−6898.
(43) Meng, L., Mohan, R., Kwok, B. H., Elofsson, M., Sin, N., and Crews, C. M. (1999) Epoxomicin, a potent and selective proteasome inhibitor, exhibits *in vivo* antiinflammatory activity. *Proc. Natl. Acad. Sci. U.S.A. 96*, 10403−10408.
(44) Arancio, O., Kiebler, M., Lee, C. J., Lev-Ram, V., Tsien, R. Y., Kandel, E. R., and Hawkins, R. D. (1996) Nitric oxide acts directly in the presynaptic neuron to produce long-term potentiation in cultured hippocampal neurons. *Cell 87*, 1025−1035.
(45) Lee, D. H., and Goldberg, A. L. (1998) Proteasome inhibitors: valuable new tools for cell biologists. *Trends Cell Biol. 8*, 397−403.
(46) Fabre, B., Lambour, T., Delobel, J., Amalric, F., Monsarrat, B., Burlet-Schiltz, O., and Bousquet-Dubouch, M. P. (2013) Subcellular distribution and dynamics of active proteasome complexes unraveled by a workflow combining in vivo complex cross-linking and quantitative proteomics. *Mol. Cell. Proteomics 12*, 687−699.
(47) Kisselev, A. F., Callard, A., and Goldberg, A. L. (2006) Importance of the different proteolytic sites of the proteasome and the efficacy of inhibitors varies with the protein substrate. *J. Biol. Chem. 281*, 8582−8590.
(48) McBride, A., and Ryan, P. Y. (2013) Proteasome inhibitors in the treatment of multiple myeloma. *Expert Rev. Anticancer Ther. 13*, 339−358.
(49) Mato, A. R., Feldman, T., and Goy, A. (2012) Proteasome inhibition and combination therapy for non-Hodgkin's lymphoma: from bench to bedside. *Oncologist 17*, 694−707.
(50) Sanman, L. E., and Bogyo, M. (2014) Activity-based profiling of proteases. *Annu. Rev. Biochem. 83*, 249−273.
(51) Nguyen, L. T., Oien, N. P., Allbritton, N. L., and Lawrence, D. S. (2013) Lipid pools as photolabile "protecting groups": design of light-activatable bioagents. *Angew. Chem., Int. Ed. 52*, 9936−9939.
(52) Dange, T., Smith, D., Noy, T., Rommel, P. C., Jurzitza, L., Cordero, R. J., Legendre, A., Finley, D., Goldberg, A. L., and Schmidt, M. (2011) Blm10 protein promotes proteasomal substrate turnover by an active gating mechanism. *J. Biol. Chem. 286*, 42830−42839.